

## The n\_TOF NEAR Station Commissioning and first physics case

M. E. Stamati<sup>1,2</sup>, P. Torres-Sánchez<sup>3,\*</sup>, P. Pérez-Maroto<sup>4</sup>, M. Cecchetto<sup>2</sup>, S. Goula<sup>1</sup>, M. Mastromarco<sup>5,6</sup>, S. Chasapoglou<sup>7</sup>, C. Beltrami<sup>8</sup>, D. Chiesa<sup>9,10</sup>, A. Manna<sup>11,12</sup>, R. Mucciola<sup>13,14</sup>, N. Patronis<sup>1</sup>, J. Praena<sup>2,3</sup>, C. Guerrero<sup>4</sup>, N. Colonna<sup>5</sup>, A. Mengoni<sup>15,11</sup>, C. Massimi<sup>11,12</sup>, O. Aberle<sup>2</sup>, V. Alcayne<sup>16</sup>, S. Altieri<sup>8,17</sup>, S. Amaducci<sup>18</sup>, H. Amar Es-Sghir<sup>3</sup>, J. Andrzejewski<sup>19</sup>, V. Babiano-Suarez<sup>20</sup>, M. Bacak<sup>2</sup>, J. Balibrea<sup>20</sup>, S. Bennett<sup>21</sup>, A. P. Bernardes<sup>2</sup>, E. Berthoumieux<sup>22</sup>, D. Bosnar<sup>23</sup>, M. Busso<sup>13,14</sup>, M. Caamaño<sup>24</sup>, F. Calviño<sup>25</sup>, M. Calviani<sup>2</sup>, D. Cano-Ott<sup>16</sup>, A. Casanovas<sup>20</sup>, D. M. Castelluccio<sup>15,11</sup>, F. Cerutti<sup>2</sup>, G. Cescutti<sup>26,27</sup>, E. Chiaveri<sup>2,21</sup>, P. Colombetti<sup>28,29</sup>, P. C. Console Camprini<sup>15,11</sup>, G. Cortés<sup>25</sup>, M. A. Cortés-Giraldo<sup>4</sup>, L. Cosentino<sup>18</sup>, S. Cristallo<sup>13,30</sup>, M. Di Castro<sup>2</sup>, D. Diacono<sup>5</sup>, M. Diakaki<sup>7</sup>, M. Dietz<sup>31</sup>, C. Domingo-Pardo<sup>20</sup>, R. Dressler<sup>32</sup>, E. Dupont<sup>22</sup>, I. Durán<sup>24</sup>, Z. Eleme<sup>1</sup>, S. Fargier<sup>2</sup>, B. Fernández-Domínguez<sup>24</sup>, P. Finocchiaro<sup>18</sup>, S. Fiore<sup>15,33</sup>, V. Furman<sup>34</sup>, F. García-Infantes<sup>3,2</sup>, A. Gawlik-Ramięga<sup>19</sup>, G. Gervino<sup>28,29</sup>, S. Gilardoni<sup>2</sup>, E. González-Romero<sup>16</sup>, F. Gunsing<sup>22</sup>, C. Gustavino<sup>33</sup>, J. Heyse<sup>35</sup>, D. G. Jenkins<sup>36</sup>, E. Jericha<sup>37</sup>, A. Junghans<sup>38</sup>, Y. Kadi<sup>2</sup>, T. Katabuchi<sup>39</sup>, I. Knapová<sup>40</sup>, M. Kokkoris<sup>7</sup>, Y. Kopatch<sup>34</sup>, M. Krtička<sup>40</sup>, D. Kurtulgil<sup>41</sup>, I. Ladarescu<sup>20</sup>, C. Lederer-Woods<sup>42</sup>, J. Lerendegui-Marco<sup>20</sup>, G. Lerner<sup>2</sup>, T. Martínez<sup>16</sup>, A. Masi<sup>2</sup>, P. Mastinu<sup>43</sup>, F. Matteucci<sup>26,27</sup>, E. A. Mauger<sup>32</sup>, A. Mazzone<sup>5,44</sup>, E. Mendoza<sup>16</sup>, V. Michalopoulou<sup>7,2</sup>, P. M. Milazzo<sup>26</sup>, F. Murtas<sup>45</sup>, E. Musacchio-Gonzalez<sup>43</sup>, A. Musumarra<sup>46,47</sup>, A. Negret<sup>46</sup>, A. Oprea<sup>48</sup>, J. A. Pavón-Rodríguez<sup>4,2</sup>, M. G. Pellegriti<sup>46</sup>, J. Perkowski<sup>19</sup>, C. Petrone<sup>48</sup>, L. Piersanti<sup>13,30</sup>, E. Pirovano<sup>31</sup>, S. Pomp<sup>49</sup>, I. Porras<sup>3</sup>, N. Protti<sup>8,17</sup>, J. M. Quesada<sup>4</sup>, T. Rauscher<sup>50</sup>, R. Reifarh<sup>41</sup>, D. Rochman<sup>32</sup>, Y. Romanets<sup>51</sup>, F. Romano<sup>46</sup>, C. Rubbia<sup>2</sup>, A. Sánchez<sup>16</sup>, M. Sabaté-Gilarte<sup>2</sup>, P. Schillebeeckx<sup>35</sup>, D. Schumann<sup>32</sup>, A. Sekhar<sup>21</sup>, A. G. Smith<sup>21</sup>, N. V. Sosnin<sup>42</sup>, M. Spelta<sup>11,12</sup>, G. Tagliente<sup>5</sup>, A. Tarifeño-Saldivia<sup>25</sup>, D. Tarrío<sup>49</sup>, N. Terranova<sup>15,45</sup>, S. Ullrich<sup>38,2</sup>, S. Valenta<sup>40</sup>, V. Variale<sup>5</sup>, P. Vaz<sup>51</sup>, D. Vescovi<sup>41</sup>, V. Vlachoudis<sup>2</sup>, R. Vlastou<sup>7</sup>, A. Wallner<sup>52</sup>, P. J. Woods<sup>42</sup>, T. Wright<sup>21</sup>, and P. Žugec<sup>23</sup>  
and the n\_TOF Collaboration

<sup>1</sup>University of Ioannina, Greece

<sup>2</sup>European Organization for Nuclear Research (CERN), Switzerland

<sup>3</sup>University of Granada, Spain

<sup>4</sup>Universidad de Sevilla, Spain

<sup>5</sup>Istituto Nazionale di Fisica Nucleare, Sezione di Bari, Italy

<sup>6</sup>Dipartimento Interateneo di Fisica, Università degli Studi di Bari, Italy

<sup>7</sup>National Technical University of Athens, Greece

<sup>8</sup>Department of Physics, University of Pavia, Italy

<sup>9</sup>Università di Milano Bicocca, Italy

<sup>10</sup>Istituto Nazionale di Fisica Nucleare, Sezione di Milano Bicocca, Milan, Italy

<sup>11</sup>Istituto Nazionale di Fisica Nucleare, Sezione di Bologna, Italy

<sup>12</sup>Dipartimento di Fisica e Astronomia, Università di Bologna, Italy

<sup>13</sup>Istituto Nazionale di Fisica Nucleare, Sezione di Perugia, Italy

<sup>14</sup>Dipartimento di Fisica e Geologia, Università di Perugia, Italy

<sup>15</sup>Agenzia nazionale per le nuove tecnologie (ENEA), Italy

<sup>16</sup>Centro de Investigaciones Energéticas Medioambientales y Tecnológicas (CIEMAT), Spain

<sup>17</sup>Istituto Nazionale di Fisica Nucleare, Sezione di Pavia, Italy

<sup>18</sup>INFN Laboratori Nazionali del Sud, Catania, Italy

<sup>19</sup>University of Lodz, Poland

<sup>20</sup>Instituto de Física Corpuscular, CSIC - Universidad de Valencia, Spain

<sup>21</sup>University of Manchester, United Kingdom

<sup>22</sup>CEA Irfu, Université Paris-Saclay, F-91191 Gif-sur-Yvette, France

<sup>23</sup>Department of Physics, Faculty of Science, University of Zagreb, Zagreb, Croatia

<sup>24</sup>University of Santiago de Compostela, Spain

<sup>25</sup>Universitat Politècnica de Catalunya, Spain

<sup>26</sup>Istituto Nazionale di Fisica Nucleare, Sezione di Trieste, Italy

<sup>27</sup>Department of Physics, University of Trieste, Italy

<sup>28</sup>Istituto Nazionale di Fisica Nucleare, Sezione di Torino, Italy

<sup>29</sup>Department of Physics, University of Torino, Italy

<sup>30</sup>Istituto Nazionale di Astrofisica - Osservatorio Astronomico di Teramo, Italy

<sup>31</sup>Physikalisch-Technische Bundesanstalt (PTB), Bundesallee 100, 38116 Braunschweig, Germany

<sup>32</sup>Paul Scherrer Institut (PSI), Villigen, Switzerland

- <sup>33</sup>Istituto Nazionale di Fisica Nucleare, Sezione di Roma1, Roma, Italy  
<sup>34</sup>Joint Institute for Nuclear Research (JINR), Dubna, Russia  
<sup>35</sup>European Commission, Joint Research Centre (JRC), Geel, Belgium  
<sup>36</sup>University of York, United Kingdom  
<sup>37</sup>TU Wien, Atominstytut, Stadionallee 2, 1020 Wien, Austria  
<sup>38</sup>Helmholtz-Zentrum Dresden-Rossendorf, Germany  
<sup>39</sup>Tokyo Institute of Technology, Japan  
<sup>40</sup>Charles University, Prague, Czech Republic  
<sup>41</sup>Goethe University Frankfurt, Germany  
<sup>42</sup>School of Physics and Astronomy, University of Edinburgh, United Kingdom  
<sup>43</sup>INFN Laboratori Nazionali di Legnaro, Italy  
<sup>44</sup>Consiglio Nazionale delle Ricerche, Bari, Italy  
<sup>45</sup>INFN Laboratori Nazionali di Frascati, Italy  
<sup>46</sup>Istituto Nazionale di Fisica Nucleare, Sezione di Catania, Italy  
<sup>47</sup>Department of Physics and Astronomy, University of Catania, Italy  
<sup>48</sup>Horia Hulubei National Institute of Physics and Nuclear Engineering, Romania  
<sup>49</sup>Uppsala University, Sweden  
<sup>50</sup>Department of Physics, University of Basel, Switzerland  
<sup>51</sup>Instituto Superior Técnico, Lisbon, Portugal  
<sup>52</sup>Australian National University, Canberra, Australia

**Abstract.** The NEAR Station is a new experimental area developed at the n\_TOF Facility at CERN. The activation station of NEAR underwent a characterization of the beam following the installation of the new n\_TOF Spallation Target. The commissioning of the neutron beam comprises a set of simulations made with the FLUKA code and experimental verification. The experimental determination of the neutron spectrum was made using activation techniques with three separate set-ups. Two set-ups were based on the Multi-foil Activation technique (MAM-1 and MAM-2), and the third set-up relied on the process of neutron moderation and activation of a single material (ANTILoPE). The three set-ups are presented. Also the present plans and future perspectives of the activation station of NEAR are discussed.

## 1 Introduction

The n\_TOF facility is CERN's pulsed neutron source. It is based on a 20 GeV/c proton beam, delivered by the PS accelerator, impinging on a lead spallation target installed inside a shielded bunker. During CERN's Long Shutdown 2 (2019-2021), the shielding was opened and completely overhauled in order to allow easier access to the target, which was replaced with a new generation one. In parallel, an experimental area named "NEAR" Station was designed and developed[1]. The NEAR Station comprises two sub-areas, the irradiation station (i-NEAR), located next to the target, and the activation station (a-NEAR) located outside the shielding, approximately 3 meters from the target[2]. The aim of the NEAR experimental area is to study the effect of radiation on materials and electronics as well as to perform cross-section measurements via the activation technique. In this work, the focus is on a-NEAR and more specifically the determination of its experimental conditions through simulations and experimental data. Furthermore, the future perspectives of the station will be briefly described.

## 2 Commissioning

The characterization of the neutron beam and experimental conditions at the NEAR is challenging as the neutron spectrum is difficult to measure via the TOF technique due to the short distance from the collimator, also given the

wide-energy spectrum covering from meV to over hundreds of MeV. In addition, the harsh radiation conditions make it difficult to measure the spectrum with standard on-line detectors and electronics. To this aim, a set of off-line strategies for measuring the neutron flux at the exit of the NEAR collimator were brought together. These were based on activation techniques, probing the full spectrum of interest in the NEAR Station by using several different materials (Multi-foil Activation Measurements, MAM), or a single material underneath a moderating device. These first measurements serve as best candidates both for characterizing the neutron beam and for testing the experimental capabilities and of work-flow of the NEAR Station.

### 2.1 Simulations

FLUKA Monte Carlo simulations [3–5] were performed to retrieve the neutron flux and the homogeneity of the incoming beam. The neutron spectrum within a radius of 4 cm with respect to the collimator centre is shown in Figure 1. As it can be noticed, the thermal neutron flux is low in this area because most of neutrons (with high energy) come directly from the target, and hence, neutron scattering is limited.

The horizontal beam profile on the same position is depicted in Figure 2, which highlights that only between a radius of about 2 cm the neutron flux is essentially constant, while at a distance of 4 cm is already several factors lower. Moreover, Figure 2 puts in evidence that the beam profile is not perfectly symmetric but a slight shift can be observed to the right (negative coordinate). This out-

\*e-mail: pablotorres@ugr.es

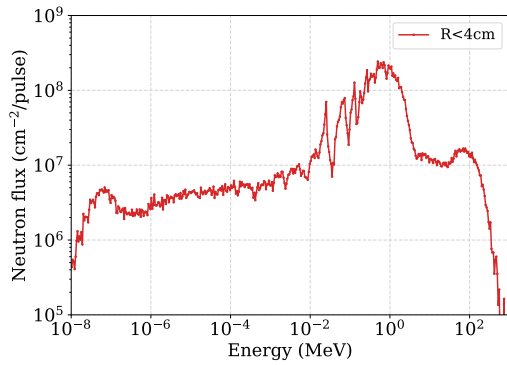


Figure 1: Neutron spectrum considering a radius of 4 cm on the external surface of the marble shielding normalized per pulse, which corresponds to  $7 \cdot 10^{12}$  protons on target.

come is better seen in the 2D homogeneity map of Figure 3, which emphasizes a slightly higher flux on the top-left of the collimator output.

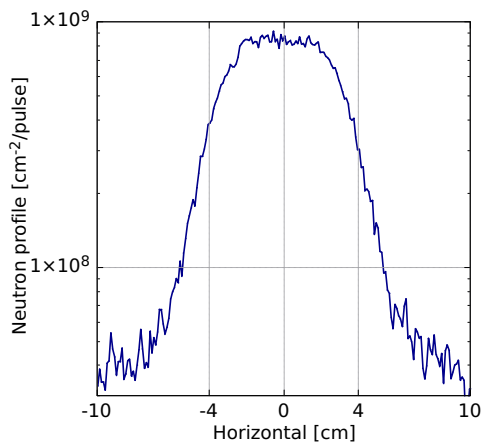


Figure 2: Neutron beam profile in the horizontal direction normalized per pulse.

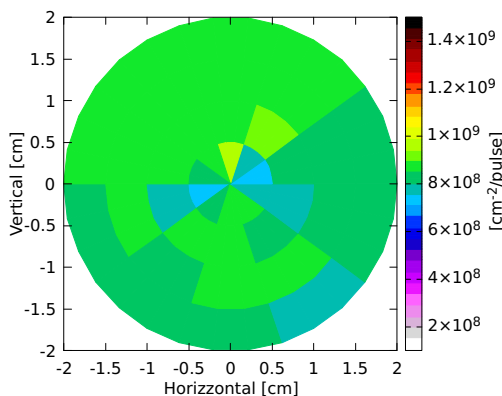


Figure 3: Homogeneity map of the beam within 2 cm of radius from the centre.

## 2.2 Multi-foil Activation Measurements (MAM)

The Multi-foil Activation Technique is based on the use of a set of materials whose response to neutrons is different depending on the energy range of the neutrons. The neutron beam under study is used to irradiate the foils, activating the material by producing a series of radioactive nuclides, whose activity can be subsequently measured by Gamma Spectroscopy. The production of an isotope ( $N_j$ ) after neutron irradiation is controlled by the overlap between the production reaction cross-section of the isotope ( $\sigma_j$ ) and the fluence spectrum ( $\Phi$ ), following the equation:

$$N_j = n_j \int \tilde{\Phi}_j(E)\sigma_j(E)dE = n_j \int \Phi(E)\kappa_j(E)\sigma_j(E)dE \quad (1)$$

where  $n_j$  is the amount of parent nuclei in the sample, and index  $j$  runs over all the produced isotopes of interest. In reality, the neutron fluence noticed by the foil  $\tilde{\Phi}_j$  is not the same as the neutron fluence under free-air conditions,  $\Phi$ , due to the presence of effects that disturb the beam, accounted by a factor  $\kappa_j$ , mainly the neutron interaction within the foil itself, that attenuates and scatters along the foil, but also the beam changes provoked by surrounding materials (e.g. another foils or scattering off the support). The activation information obtained by Gamma Spectroscopy of the irradiated samples can be then used to reconstruct the spectrum. This can be performed using the matrix form of the previous expression:

$$N_j = \sum_i R_{ij}\Phi_i \quad (2)$$

where  $R_{ij}$  are the elements of the response matrix and  $\Phi_i$  are the corresponding flux at each energy interval. An unfolding procedure can then be used to obtain the flux.

## 2.3 Neutron Moderation Spectrometer

Another approach is the use of a moderator to slow down the neutrons before they are captured in the irradiated foils. Only one activation material (and therefore, one reaction cross-section) is used in this technique, so the response of the foils to a certain neutron energy depends on the amount of material needed to stop it before its capture. After the irradiation, the activation of each foil is measured to obtain the number of captures  $N_i$ . This quantity is related to the discretized neutron flux  $\Phi_i$  through the so-called response matrix  $R_{ij}$  through a relation similar to equation (2).  $R_{ij}$  is obtained by simulating the response of the detector, in this case with GEANT4[6]. By solving the inverse problem with unfolding techniques it is possible to obtain the original flux  $\Phi_j$ .

The widely used Bonner Spheres Spectrometer[7] is based on this principle, but because of the characteristics of NEAR it is not practical to use them. A device called ANTILoPE (A NeuTron multi-foIL sPEctrometer) has been designed for this matter.

## 2.4 Experimental Set-ups

### 2.4.1 MAM-1

MAM-1 was one of the two set-ups used for the unfolding of the neutron energy distribution via the Multi-foil activation technique as discussed in 2.2. A detailed list of the samples that were used together with the reactions studied for each can be found in Table 1.

Table 1: Samples and reactions used for the flux extraction using MAM1

Sample ID	Mass [g]	Reactions studied
Cd	1.0714	$^{114}\text{Cd}(n,\gamma)^{115}\text{Cd}$
Sc	0.0073	$^{45}\text{Sc}(n,\gamma)^{46}\text{Sc}$
Au-1	0.0709	$^{197}\text{Au}(n,\gamma)^{198}\text{Au}$ , $^{197}\text{Au}(n,2n)^{196}\text{Au}$ , $^{197}\text{Au}(n,4n)^{194}\text{Au}$
Au-2	0.0712	$^{197}\text{Au}(n,\gamma)^{198}\text{Au}$ , $^{197}\text{Au}(n,2n)^{196}\text{Au}$ , $^{197}\text{Au}(n,4n)^{194}\text{Au}$
Au-6	0.0550	$^{197}\text{Au}(n,2n)^{196}\text{Au}$
Au-3	0.0142	$^{197}\text{Au}(n,\gamma)^{198}\text{Au}$ , $^{197}\text{Au}(n,2n)^{196}\text{Au}$
Au-4	0.0149	$^{197}\text{Au}(n,\gamma)^{198}\text{Au}$ , $^{197}\text{Au}(n,2n)^{196}\text{Au}$
Au-b	0.0148	$^{197}\text{Au}(n,\gamma)^{198}\text{Au}$ , $^{197}\text{Au}(n,2n)^{196}\text{Au}$
W	1.2349	$^{186}\text{W}(n,\gamma)^{187}\text{W}$
In	0.4675	$^{113}\text{In}(n,\gamma)^{114}\text{In}$
Ni	0.5624	$^{58}\text{Ni}(n,p)^{58}\text{Co}$ , $^{58}\text{Ni}(n,2n)^{57}\text{Ni}$
Al	0.1694	$^{27}\text{Al}(n,\alpha)^{24}\text{Na}$
Co	0.0348	$^{59}\text{Co}(n,\gamma)^{60}\text{Co}$ , $^{59}\text{Co}(n,2n)^{58}\text{Co}$ , $^{59}\text{Co}(n,3n)^{57}\text{Co}$
Bi	1.1070	$^{209}\text{Bi}(n,3n)^{207}\text{Bi}$ , $^{209}\text{Bi}(n,4n)^{206}\text{Bi}$ , $^{209}\text{Bi}(n,5n)^{205}\text{Bi}$

The samples were placed in two identical Aluminium holders, positioned inside a circular surface of 4cm diameter, which corresponds to the homogeneous part of the neutron beam. The two holders were then put in beam one behind the other, approximately 20 cm from the collimator exit, as can be seen in Fig. 4(a).

Following the irradiation, the induced activity of the samples was measured with a HPGe detector. An example of an activation spectrum is given in Figure 5. From the activation spectra, the production rate of each nuclei of interest can be extracted and then used in an unfolding code. The code used in the case of MAM1 is BaTMAN, details on which can be found in [8–10].

### 2.4.2 MAM-2

MAM-2 was another set-up designed to extract information about the beam exiting the NEAR collimator. The MAM-2 set-up consisted in a set of nine positions where



(a) MAM1 set-up

(b) MAM2 set-up

Figure 4: The two experimental set-ups used for the Multi-activation fluence extraction placed in front of the collimator exit, while being aligned with the help of lasers.

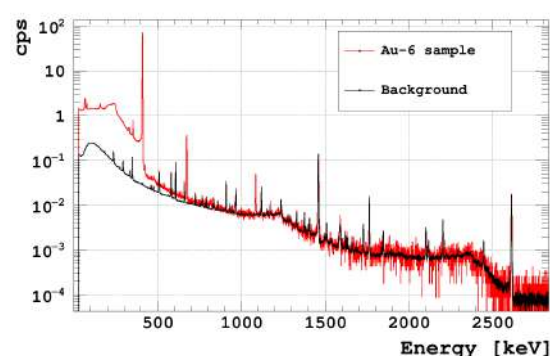


Figure 5: Activation spectrum, in counts per second, for the Au-6 foil (in black). A background spectrum is also shown (in red).

the activation samples were placed. Figure 4(b), shows a picture of the MAM-2 set-up. The central position included a stack of foils in order to characterize the spectrum using the Multi-foil activation technique. The materials used in the stack were Au, Co, Sc, In, Al and Au (upstream to downstream). Table 2 shows the list of samples and reactions used in the MAM-2 set-up. Two Au samples were used in the first and last positions in order to use the black-resonance technique in the aim to improve the energy resolution. The other 8 positions, corresponding to the edges and corners of the sample holder, had an Au sample. These samples were used to characterize the beam spatial homogeneity at three energies corresponding to the three reactions measured from Au ( $^{197}\text{Au}(n,\gamma)$ ,  $^{197}\text{Au}(n,2n)$  and  $^{197}\text{Au}(n,4n)$ ). The edges and corners were located at 3.13 and 4.17 cm from the center, respectively. All of the samples were covered in the downstream position with a cadmium cover, in order to avoid thermal neutron contamination from scattered neutrons in the surrounding materials and walls.

After irradiation, the samples were measured by Gamma Spectroscopy with a HPGe detector at several times in order to extract the activity of the samples, given the broad range of half-lives of the measured isotopes. Figure 6 shows some of the Gamma Spectra obtained from the measurement of the samples in the central stack. The ac-

Table 2: The samples and reactions used for the MAM-2 set-up. All the Au samples labeled with number correspond to the homogeneity analysis. For these samples, the three reactions ( $^{197}\text{Au}(n,\gamma)$ ,  $^{197}\text{Au}(n,2n)$ ,  $^{197}\text{Au}(n,4n)$ ) were also used.

Sample ID	Mass [g]	Reactions studied
Au-u	0.1268	$^{197}\text{Au}(n,\gamma)^{198}\text{Au}$ , $^{197}\text{Au}(n,2n)^{196}\text{Au}$ , $^{197}\text{Au}(n,4n)^{194}\text{Au}$
Co	0.0644	$^{59}\text{Co}(n,\gamma)^{60}\text{Co}$ , $^{59}\text{Co}(n,2n)^{58}\text{Co}$ , $^{59}\text{Co}(n,3n)^{57}\text{Co}$ , $^{59}\text{Co}(n,4n)^{56}\text{Co}$ , $^{59}\text{Co}(n,p)^{59}\text{Fe}$
Sc	0.0503	$^{45}\text{Sc}(n,\gamma)^{46}\text{Sc}$
In	0.1309	$^{113}\text{In}(n,3n)^{111}\text{In}$ , $^{113}\text{In}(n,4n)^{110}\text{In}$ , $^{115}\text{In}(n,n')^{115m}\text{In}$
Al	0.2552	$^{27}\text{Al}(n,\alpha)^{24}\text{Na}$
Au-d	0.1283	$^{197}\text{Au}(n,\gamma)^{198}\text{Au}$ , $^{197}\text{Au}(n,2n)^{196}\text{Au}$ , $^{197}\text{Au}(n,4n)^{194}\text{Au}$
Au-1	0.1167	
Au-2	0.1213	
Au-3	1.1154	
Au-4	0.1214	$^{197}\text{Au}(n,\gamma)^{198}\text{Au}$ ,
Au-6	0.1257	$^{197}\text{Au}(n,2n)^{196}\text{Au}$ ,
Au-7	0.1250	$^{197}\text{Au}(n,4n)^{194}\text{Au}$
Au-8	0.1243	
Au-9	0.1222	

tivation data is then used as input for the unfolding of the spectrum, performed using a Bayesian strategy. The code JAGS for analysis of Bayesian models was used [11], following the design described in Ref. [9].

### 2.4.3 ANTILoPE

ANTILoPE is the third device designed to measure the neutron flux at the NEAR station. The detector is basically a  $15 \times 15 \times 30 \text{ cm}^3$  polyethylene block to moderate the neutrons, inside which a certain number of foils can be inserted at different positions. Since the capture cross section is a standard and the decay characteristics of the  $^{198}\text{Au}$  are suitable for an optimal activation measurement,  $^{197}\text{Au}$  was the material chosen for the foils. 20 foils were included into the set-up for the NEAR campaign, as can be seen in Fig. 7 (left). In addition, a  $10 \times 10 \times 2 \text{ cm}^3$  Pb block was added to improve the sensitivity to fast neutrons. A 1 mm thick layer of Cd surrounds the whole set-up to protect ANTILoPE from capturing scattered neutrons. The device was placed just after the NEAR collimator for the irradiation, in the position shown in Fig. 7 (right).

After the irradiation, the activity of the foils was measured with a couple of  $\text{LaBr}_3$  detectors. The number of neutron captures per mg in the foils is given in Fig. 8, along with the expected value obtained by simulations. An

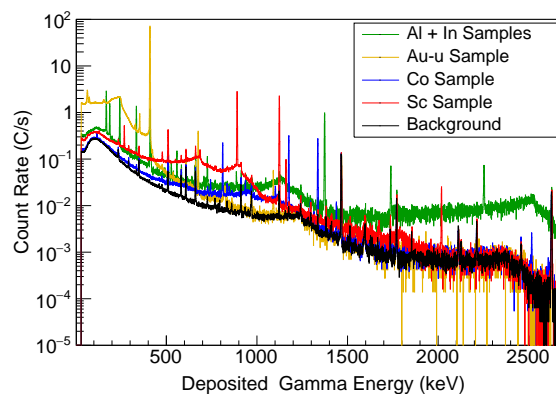


Figure 6: Gamma spectroscopy measurements for the samples in the central position of the MAM-2 set-up. The Al and In samples were measured together in order to obtain data on three short lived isotopes ( $^{24}\text{Na}$ ,  $t_{1/2} = 15 \text{ h}$ ;  $^{110}\text{In}$ ,  $t_{1/2} = 4.92 \text{ h}$  and  $^{115m}\text{In}$ ,  $t_{1/2} = 4.486 \text{ h}$ ).



Figure 7: Distribution of the gold foils inside ANTILoPE together with the Pb block (right) and the complete set-up placed just after the NEAR collimator (left).

agreement within 5% is found in the first 15 foils, with some discrepancies observed in the last ones. This might be due because of a higher contribution of scattering neutrons coming back from the experimental hall and the difficulty of simulating neutrons with such a high energy, which are the ones being captured at the end of the detector. Nevertheless a good agreement is found between simulations and measurements.

At the moment, investigations regarding the unfolding methodology are ongoing to ensure an appropriate neutron flux calculation. The unfolding will be performed with the code RooUnfold[12].

## 3 Present Plans and Future Perspectives

The very high instantaneous flux of the NEAR station makes it an excellent candidate for performing measurements that are too challenging or even impossible to be studied with the time-of-flight technique in  $n_{\text{TOF}}$ 's two experimental areas, especially in terms of signal-to-background ratio. For those cases, integral measurements can be performed at NEAR.

One particular category of measurements that can be aided by the NEAR station is Maxwellian averaged cross section (MACS) measurements of relevance for nuclear astrophysics. About half of the elements heavier than iron

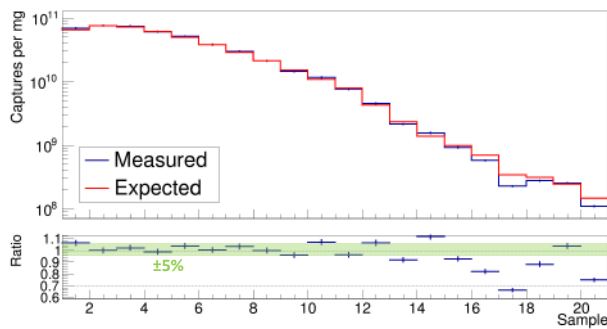


Figure 8: Comparison between the number of captures per mg in each foil and the expected value simulated with GEANT4 using the FLUKA estimated neutron flux.

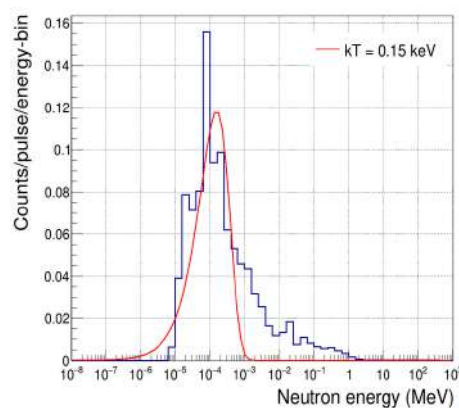


Figure 9: In blue: Neutron energy distribution after placing a 5 mm thick  $B_4C$  filter in beam. In red: A Maxwellian fit of the energy distribution.

are created through a series of neutron captures on seed nuclei and subsequent beta decays, a process known as the "slow" process (s-process)[13, 14]. This astrophysical process takes place in stars that are in thermodynamic equilibrium thus the velocity of neutrons follows a Maxwell-Boltzmann distribution[15]. With neutrons of velocities following a Maxwell-Boltzmann distribution and a reaction integral measurement, we can then determine MACS directly in the lab.

As seen from the NEAR station commissioning preliminary results, the neutron beam of NEAR is not a Maxwellian. However, with the use of proper filters in terms of material and dimensions, the neutrons' energy distribution can be "shaped" to resemble a Maxwellian spectrum. A feasibility study to confirm this possibility is being currently carried out, with the use of  $^{10}B$  enriched  $B_4C$  disks of different thicknesses used as filters. The results of a simulated flux after 5mm of  $B_4C$  can be seen in Figure 9.

## 4 Conclusions

During CERN's Long Shutdown 2 phase of 2019-2021, a new high-flux irradiation station, the NEAR Station, was

designed and developed in the n\_TOF facility. In order to explore its experimental conditions, both simulations and experimental measurements were carried out. The simulations were performed with the FLUKA code while the experimental measurements were carried out with the activation technique using three independent set-ups based on different principles, two of them on the multi-foil activation method and one of them on neutron moderation. The features of the set-ups used for those measurements were presented above. Following the commissioning measurements, a new experimental campaign has been launched in order to investigate the possibility of shaping the NEAR neutron energy distribution into a Maxwellian-like spectrum, opening the way to MACS integral measurements at n\_TOF.

## References

- [1] A. Mengoni, the n\_TOF Collaboration, Tech. rep. (2020), <http://cds.cern.ch/record/2737308/files/INTC-I-222.pdf>
- [2] M. Ferrari, D. Senajova, O. Aberle, Y. Aguiar, D. Baillard, M. Barbagallo, A.P. Bernardes, L. Buonocore, M. Cecchetto, V. Clerc et al., *Design development and implementation of an irradiation station at the neutron time-of-flight facility at cern* (2022), <https://arxiv.org/abs/2202.12809>
- [3] <https://fluka.cern>
- [4] V. Vlachoudis, *Flair: A powerful but user friendly graphical interface for FLUKA* (American Nuclear Society - ANS, United States, 2009), ISBN 978-0-89448-069-0, [http://inis.iaea.org/search/search.aspx?orig\\_q=RN:42064858](http://inis.iaea.org/search/search.aspx?orig_q=RN:42064858)
- [5] G. Battistoni, and et al., *Annals Nucl. Energy* **82**, 10 (2015)
- [6] J. Allison, K. Amako, J. Apostolakis, H. Araujo, P.A. Dubois, M. Asai, G. Barrand, R. Capra, S. Chauvie, R. Chytracsek et al., *IEEE Transactions on nuclear science* **53**, 270 (2006)
- [7] A. Alevra, D. Thomas, *Radiation Protection Dosimetry* **107**, 33 (2003)
- [8] D. Chiesa, M. Nastasi, C. Cazzaniga, M. Rebai, L. Arcidiacono, E. Previtali, G. Gorini, C.D. Frost, *Nuclear Instruments and Methods in Physics Research Section A: Accelerators, Spectrometers, Detectors and Associated Equipment* **902**, 14 (2018)
- [9] D. Chiesa, E. Previtali, M. Sisti, *Annals of Nuclear Energy* **70**, 157 (2014)
- [10] <https://github.com/davidechiesa/BaTMAN>
- [11] M. Plummer, *JAGS Version 4.3.0 user manual* (2017), <https://martynplummer.wordpress.com/2017/07/18/jags-4-3-0-is-released/>
- [12] *RooUnfold repository*, <https://gitlab.cern.ch/RooUnfold/RooUnfold>
- [13] N. Nishimura, R. Hirschi, T. Rauscher, A.S.J. Murphy, G. Cescutti, *Monthly Notices of the Royal Astronomical Society* **469**, 1752 (2017)
- [14] G. Cescutti, R. Hirschi, N. Nishimura, J.W. den Hartogh, T. Rauscher, A.S.J. Murphy, S. Cristallo,

Monthly Notices of the Royal Astronomical Society  
**478**, 4101 (2018)

[15] E.M. Burbidge, G.R. Burbidge, W.A. Fowler,  
F. Hoyle, *Reviews of Modern Physics* **29**, 547 (1957)